Collective Inference on Markov Models for Modeling Bird Migration*

Daniel Sheldon
dsheldon@cs.cornell.edu

M. A. Saleh Elmohamed
saleh@cam.cornell.edu

Dexter Kozen
kozen@cs.cornell.edu

Abstract

We investigate a family of inference problems on Markov models, where many sample paths are drawn from a Markov chain and partial information is revealed to an observer who attempts to reconstruct the sample paths. We present algorithms and hardness results for several variants of this problem which arise by revealing different information to the observer and imposing different requirements for the reconstruction of sample paths. Our algorithms are analogous to the classical Viterbi algorithm for Hidden Markov Models, which finds single most probable sample path given a sequence of observations. Our work is motivated by an important application in ecology: inferring bird migration paths from a large database of observations.

1 Introduction

Hidden Markov Models (HMMs) assume a generative model for sequential data whereby a sequence of states (or *sample path*) is drawn from a Markov chain in a hidden experiment. Each state generates an output symbol from alphabet Σ, and these output symbols constitute the data or *observations*. A classical problem, solved by the Viterbi algorithm, is to find the most probable sample path given the observations for a given Markov model. We call this the *single path problem*; it is well suited to labeling or tagging a single sequence of data. For example, HMMs have been successfully applied in speech recognition [1], natural language processing [2], and biological sequencing [3].

We introduce two generalizations of the single path problem for performing *collective inference* on Markov models, motivated by an effort to model bird migration patterns using a large database of static observations. The eBird database hosted by the Cornell Lab of Ornithology contains millions of bird observations from throughout North America, reported by the general public using the eBird web application[1]. Observations report location, date, species and number of birds observed. The eBird data set is very rich; the human eye can easily discern migration patterns from animations showing the observations as they unfold over time on a map of North America[2]. However, the eBird data are *static*, and they do not explicitly record movement, only the distributions at different points in time. Conclusions about migration patterns are made by the human observer. Our goal is to build a mathematical framework to infer dynamic migration models from the static eBird data. Quantitative migration models are of great scientific and practical import: for example, this problem arose out of an interdisciplinary project at Cornell University to model the possible spread of avian influenza in North America through wild bird migration.

The migratory behavior for a species of birds can be modeled as a single generative process that independently governs how individual birds fly between locations, giving rise to the following in-

*This work was supported in part by ONR Grant N00014-01-1-0968 and by NSF grant CCF-0635028. The views and conclusions herein are those of the authors and do not necessarily represent the official policies or endorsements of these organizations or the US Government.

[1] `http://ebird.org`

[2] `http://www.avianknowledge.net/visualization`

ference problem: a hidden experiment simultaneously draws many independent sample paths from a Markov chain, and the observations reveal aggregate information about the collection of sample paths at each time step. For example, the eBird data estimate the geographical distribution of a species on successive days, but do not track individual birds.

We discuss two problems within this framework. In the *multiple path problem*, we assume that M independent sample paths are simultaneously drawn from a Markov model, and the observations reveal the number of paths that output symbol α at time t, for each α and t. The observer seeks the most likely collection of paths given the observations. The *fractional path problem* is a further generalization in which paths are divisible entities. The observations reveal the fraction of paths that output symbol α at time t, and the observer's job is to find the most likely (in a sense to be defined later) weighted collection of paths given the observations. Conceptually, the fractional path problem can be derived from the multiple path problem by letting M go to infinity; or it has a probabilistic interpretation in terms of distributions over paths.

After discussing some preliminaries in section 2, sections 3 and 4 present algorithms for the multiple and fractional path problems, respectively, using network flow techniques on the *trellis graph* of the Markov model. The multiple path problem in its most general form is NP-hard, but can be solved as an integer program. The special case when output symbols uniquely identify their associated states can be solved efficiently as a flow problem; although the single path problem is trivial in this case, the multiple and fractional path problems remain interesting. The fractional path problem can be solved by linear programming. In section 5, we present preliminary results on migration inference for *Archilochus colubris*, the Ruby-throated Hummingbird, devoting some attention to a challenging problem we have neglected so far: estimating species distributions from eBird observations. We also introduce a few practical extensions to the fractional paths problem, including slack variables allowing the solution to deviate slightly from potentially noisy observations.

We briefly mention some related work. Caruana et al. [4] and Phillips et al. [5] used machine learning techniques to model bird distributions from observations and environmental features. For problems on sequential data, many variants of HMMs have been proposed [3], and recently, conditional random fields (CRFs) have become a popular alternative [6]. Roth and Yih [7] present an integer programming inference framework for CRFs that is similar to our problem formulations.

2 Preliminaries

2.1 Data Model and Notation

A Markov model (V, p, Σ, σ) is a Markov chain with state set V and transition probabilities $p(u, v)$ for all $u, v \in V$. Each state generates a unique output symbol from alphabet Σ, given by the mapping $\sigma : V \to \Sigma$. Although some presentations allow each state to output multiple symbols with different emission probabilities, we lose no generality assuming that each state emits a unique symbol — to encode a model where state v output multiple symbols, we simply duplicate v for each symbol and encode the emission probabilities into the transitions. Of course, σ need not be one-to-one. It is useful to think of σ as a partition of the states, letting $V_\alpha = \sigma^{-1}(\alpha)$ be the set of all states that output α. We assume each model has a distinguished start state s and output symbol `start`.

Let $\mathcal{Y} = V^T$ be the set of all possible sample paths of length T. We represent a path $\mathbf{y} \in \mathcal{Y}$ as a row vector $\mathbf{y} = (y_1, \ldots, y_T)$, and a collection of M paths as the $M \times T$ matrix $\mathbf{Y} = (y_{it})$, with each row $\mathbf{y}_{i\cdot}$ representing an independent sample path. The transition probabilities induce a distribution λ on $\mathcal{Y}$, where $\lambda(\mathbf{y}) = \prod_{t=1}^{T-1} p(y_t, y_{t+1})$. We will also consider arbitrary distributions π over $\mathcal{Y}$, letting $Y = (Y_1, \ldots, Y_T)$ denote a random path from π. Then, for example, we write $\Pr_\pi [Y_t = u]$ to be the probability under π that the tth state is u, and $E_\pi [f(Y)]$ to be the expected value of $f(Y)$ for any function f of a random path Y drawn from π. Note that $\mathbf{Y}$ (boldface) denotes a matrix of M paths, while Y denotes a random path.

2.2 The Trellis Graph and Viterbi as Shortest Path

To develop our flow-based algorithms, it is instructive to build upon a shortest-path interpretation of the Viterbi algorithm [7]. In an instance of the single path problem we are given a model (V, p, Σ, σ) and observations $\alpha_1, \ldots, \alpha_T$, and we seek the most probable path $\mathbf{y}$ given the observations. We call

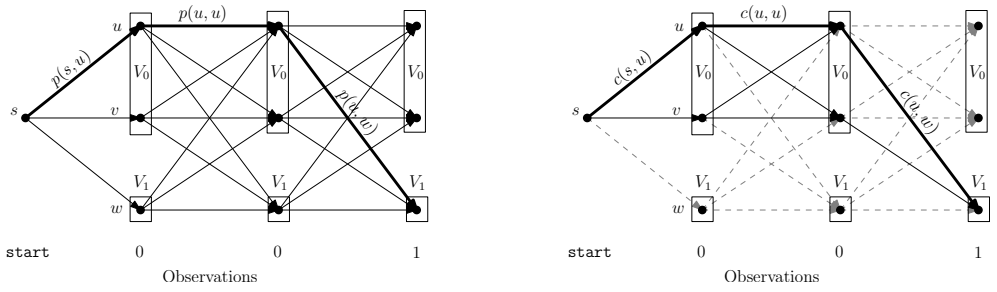

(a) (b)

Figure 1: Trellis graph for Markov model with states $\{s, u, v, w\}$ and alphabet $\{\texttt{start}, 0, 1\}$. States u and v output the symbol 0, and state w outputs the symbol 1. (a) The bold path is feasible for the specified observations, with probability $p(s,u)p(u,u)p(u,w)$. (b) Infeasible edges have been removed (indicated by light dashed lines), and probabilities changed to costs. The bold path has cost $c(s,u) + c(u,u) + c(u,w)$.

path $\mathbf{y}$ *feasible* if $\sigma(y_t) = \alpha_t$ for all t; then we wish to maximize $\lambda(\mathbf{y})$ over feasible $\mathbf{y}$. The problem is conveniently illustrated using the *trellis graph* of the Markov model (Figure 1). Here, the states are replicated for each time step, and edges connect a state at time t to its possible successors at time $t+1$, labeled with the transition probability. A feasible path must pass through partition V_{α_t} at step t, so we can prune all edges incident on other partitions, leaving only feasible paths. By defining the cost of an edge as $c(u,v) = -\log p(u,v)$, and letting the path cost $c(\mathbf{y})$ be the sum of its edge costs, straightforward algebra shows that $\arg\max_{\mathbf{y}} \lambda(\mathbf{y}) = \arg\min_{\mathbf{y}} c(\mathbf{y})$, i.e., the path of maximum probability becomes the path of minimum cost under this transformation. Thus the Viterbi algorithm finds the shortest feasible path in the trellis using edge lengths $c(u,v)$.

3 Multiple Path Problem

In the multiple path problem, M sample paths are drawn from the model and the observations reveal the number of paths $N_t(\alpha)$ that output α at time t, for all α and t; or, equivalently, the multiset A_t of output symbols at time t. The objective is to find the most probable collection $\mathbf{Y}$ that is feasible, meaning it produces multisets $A_1, \ldots, A_T$. The probability $\lambda(\mathbf{Y})$ is just the product of the path-wise probabilities:

$$\lambda(\mathbf{Y}) = \prod_{i=1}^{M} \lambda(\mathbf{y}_i) = \prod_{i=1}^{M} \prod_{t=1}^{T-1} p(y_{i,t}, y_{i,t+1}). \tag{1}$$

Then the formal specification of this problem is

$$\max_{\mathbf{Y}} \lambda(\mathbf{Y}) \text{ subject to } |\{i : y_{i,t} \in V_\alpha\}| = N_t(\alpha) \text{ for all } \alpha, t. \tag{2}$$

3.1 Reduction to the Single Path Problem

A naive approach to the multiple path problem reduces it to the single path problem by creating a new Markov model on state set V^M where state $\langle v_1, \ldots, v_M \rangle$ encodes an entire tuple of original states, and the transition probabilities are given by the product of the element-wise transition probabilities:

$$p(\langle u_1, \ldots, u_M \rangle, \langle v_1, \ldots, v_M \rangle) = \prod_{i=1}^{M} p(u_i, v_i).$$

A state from the product space V^M corresponds to an entire column of the matrix $\mathbf{Y}$, and by changing the order of multiplication in (1), we see that the probability of a path in the new model is equal to the probability of the entire collection of paths in the old model. To complete the reduction, we form a new alphabet $\hat{\Sigma}$ whose symbols represent multisets of size M on Σ. Then the solution to (2) can be found by running the Viterbi algorithm to find the most likely sequence of states from V^M that produce output symbols (multisets) $A_1, \ldots, A_T$. The running time is polynomial in $|V^M|$ and $|\hat{\Sigma}|$, but exponential in M.

3.2 Graph Flow Formulation

Can we do better than the naive approach? Viewing the cost of a path as the cost of routing one unit of flow along that path in the trellis, a minimum cost collection of M paths is equivalent to a minimum cost flow of M units through the trellis — given M paths, we can route one unit along each to get a flow, and we can decompose any flow of M units into paths each carrying a single unit of flow. Thus we can write the optimization problem in (2) as the following flow integer program, with additional constraints that the flow paths generate the correct observations. The decision variable x^t_{uv} indicates the flow traveling from u to v at time t; or, the number of sample paths that transition from u to v at time t.

$$\text{(IP)} \qquad \begin{aligned} \min & \sum_{u,v,t} c(u,v) x^t_{uv} \\ \text{s.t.} \quad & \sum_u x^t_{uv} = \sum_w x^{t+1}_{vw} && \text{for all } v,t, && (3) \\ & \sum_{u \in V_\alpha, v \in V} x^t_{uv} = N_t(\alpha) && \text{for all } \alpha, t, && (4) \\ & x^t_{uv} \in \mathbb{N} && \text{for all } u,v,t. \end{aligned}$$

The flow conservation constraints (3) are standard: the flow into v at time t is equal to the flow leaving v at time $t+1$. The observation constraints (4) specify that $N_t(\alpha)$ units of flow leave partition V_α at time t. These also imply that exactly M units of flow pass through each level of the trellis, by summing over all α,

$$\sum_{u,v} x^t_{uv} = \sum_\alpha \sum_{u \in V_\alpha, v \in V} x^t_{uv} = \sum_\alpha N_t(\alpha) = M.$$

Without the observation constraints, IP would be an instance of the minimum-cost flow problem [8], which is solvable in polynomial time by a variety of algorithms [9]. However, we cannot hope to encode the observation constraints into the flow framework, due to the following result.

Lemma 1. *The multiple path problem is NP-hard.*

The proof of Lemma 1 is by reduction from SET COVER, and is omitted. One may use a general purpose integer program solver to solve IP directly; this may be efficient in some cases despite the lack of polynomial time performance guarantees. In the following sections we discuss alternatives that are efficiently solvable.

3.3 An Efficient Special Case

In the special case when σ is one-to-one, the output symbols uniquely identify their generating states, so we may assume that $\Sigma = V$, and the output symbol is always the name of the current state. To see how the problem IP simplifies, we now have $V_u = \{u\}$ for all u, so each partition consists of a single state, and the observations completely specify the flow through each node in the trellis:

$$\sum_v x^t_{uv} = N_t(u) \quad \text{for all } u,t. \tag{4′}$$

Substituting the new observation constraints (4′) for time $t+1$ into the RHS of the flow conservation constraints (3) for time t yield the following replacements:

$$\sum_u x^t_{uv} = N_{t+1}(v) \quad \text{for all } v,t. \tag{3′}$$

This gives an equivalent set of constraints, each of which refers only to variables x^t_{uv} for a single t. Hence the problem can be decomposed into $T-1$ disjoint subproblems for $t = 1, \ldots, T-1$. The tth subproblem IP_t is given in Figure 2(a), and illustrated on the trellis in Figure 2(b). State u at time t has a supply of $N_t(u)$ units of flow coming from the previous step, and we must route $N_{t+1}(v)$ units of flow to state v at time $t+1$, so we place a demand of $N_{t+1}(v)$ at the corresponding node. Then the problem reduces to finding a minimum cost routing of the supply from time t to meet the demand at time $t+1$, solved separately for all $t = 1, \ldots, T-1$. The problem IP_t an instance of the transportation problem [10], a special case of the minimum-cost flow problem. There are a variety of efficient algorithms to solve both problems [8, 9], or one may use a general purpose linear program (LP) solver; any basic solution to the LP relaxation of IP_t is guaranteed to be integral [8].

$$
\begin{aligned}
(\text{IP}_t) \qquad & \min \sum_{u,v} c(u,v) x^t_{uv} \\
& \text{s.t.} \quad \sum_u x^t_{uv} = N_{t+1}(v) \qquad \forall v, \quad (3') \\
& \qquad \sum_v x^t_{uv} = N_t(u) \qquad \forall u, \quad (4') \\
& \qquad x^t_{uv} \in \mathbb{N} \qquad \forall u, v.
\end{aligned}
$$

(a)

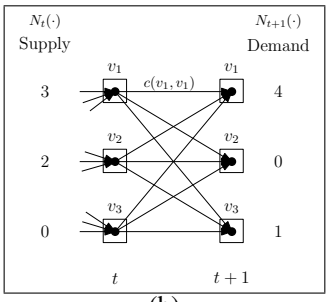

(b)

Figure 2: (a) The definition of subproblem IP_t. (b) Illustration on the trellis.

4 Fractional Paths Problem

In the fractional paths problem, a path is a divisible entity. The observations specify $q_t(\alpha)$, the fraction of paths that output α at time t, and the observer chooses $\pi(\mathbf{y})$ fractional units of each path $\mathbf{y}$, totaling one unit, such that $q_t(\alpha)$ units output α at time t. The objective is to maximize $\prod_{\mathbf{y} \in \mathcal{Y}} \lambda(\mathbf{y})^{\pi(\mathbf{y})}$. Put another way, π is a distribution over paths such that $\Pr_\pi [Y_t \in V_\alpha] = q_t(\alpha)$, i.e., q_t specifies the marginal distribution over symbols at time t. By taking the logarithm, an equivalent objective is to maximize $E_\pi [\log \lambda(Y)]$, so we seek the distribution π that maximizes the expected log-probability of a path Y drawn from π. Conceptually, the fractional paths problem arises by letting $M \to \infty$ in the multiple paths problem and normalizing to let $q_t(\alpha) = N_t(\alpha)/M$ specify the fraction of paths that output α at time t. Operationally, the fractional paths problem is modeled by the LP relaxation of IP, which routes one splittable unit of flow through the trellis.

$$
\begin{aligned}
(\text{RELAX}) \qquad & \min \sum_{u,v,t} c(u,v) x^t_{uv} \\
& \text{s.t.} \quad \sum_u x^t_{uv} = \sum_w x^{t+1}_{vw} \qquad \text{for all } v, t, \\
& \qquad \sum_{u \in V_\alpha} \sum_{v \in V} x^t_{uv} = q_t(\alpha) \qquad \text{for all } \alpha, t, \qquad (5) \\
& \qquad x^t_{uv} \geq 0 \qquad \text{for all } u, v, t.
\end{aligned}
$$

It is easy to see that a single-unit flow x corresponds to a probability distribution π. Given π, let $x^t_{uv} = \Pr_\pi [Y_t = u, Y_{t+1} = v]$; then x is a flow because the probability a path enters v at time t is equal to the probability it leaves v at time $t+1$. Conversely, given x, any path decomposition assigning flow $\pi(\mathbf{y})$ to each $\mathbf{y} \in \mathcal{Y}$ is a probability distribution because the total flow is one. In general, the decomposition is not unique, but any choice yields a distribution π with the same objective value. Furthermore, under this correspondence, x satisfies the marginal constraints (5) if and only if π has the correct marginals:

$$
\sum_{u \in V_\alpha} \sum_{v \in V} x^t_{uv} = \sum_{u \in V_\alpha} \sum_{v \in V} \Pr [Y_t = u, Y_{t+1} = v] = \sum_{u \in V_\alpha} \Pr [Y_t = u] = \Pr [Y_t \in V_\alpha] .
$$

Finally, we can rewrite the objective function in terms of paths:

$$
\sum_{u,v,t} c(u,v) x^t_{uv} = \sum_{\mathbf{y} \in \mathcal{Y}} \pi(\mathbf{y}) c(\mathbf{y}) = E_\pi [c(Y)] = E_\pi [-\log \lambda(Y)] .
$$

By switching signs and changing from minimization to maximization, we see that RELAX solves the fractional paths problem. This problem is very similar to maximum entropy or minimum cross entropy modeling, but the details are slightly different: such a model would typically find the distribution π with the correct marginals that minimizes the cross entropy or Kullback-Leibler divergence [11] between λ and π, which, after removing a constant term, reduces to minimizing $E_\lambda [-\log \pi(Y)]$. Like IP, the RELAX problem also decomposes into subproblems in the case when σ is one-to-one.

5 Modeling Bird Migration

Launched in 2002, eBird is one of several *citizen science* projects run by the Cornell Lab of Ornithology, designed to leverage the data gathering power of the public while educating and engaging citizen scientists on bird conservation issues. On the eBird website, birdwatchers submit checklists of birds they observe during an outing, indicating the number of birds for each species, along with the location, date, time, and some additional information. Our data set consists of the $428{,}648$ *complete* checklists from 1995 through 2007, meaning the reporter listed all species observed. This means we can infer a count of zero, or a *negative observation*, for any species not listed. Using a USGS land cover map image of North America, we preprocess the data to assign each observation to the pixel in which it occurred. The map is 615×600 pixels, with each pixel approximately 15 km on a side. All years of data are aggregated into one.

Our migration inference consists of two parts: (1) using eBird data to estimate species distributions during successive time periods and (2) inferring migration paths from species distributions using the fractional paths problem. For both problems, we divide the map into grid cells that are 15 pixels on a side and divide the year into weeks, letting our state set U be the set of all grid cells with at least 10% land mass (non-water pixels) and letting $t = 1, \ldots, 52$ represent the week of the year. We report preliminary results for *Archilochus colubris*, the Ruby-throated Hummingbird, chosen as a common bird with relatively good eBird coverage. Armed with little reference data, our evaluation is largely manual, producing maps and animations for comparison with known range maps and written accounts of migration.

5.1 Estimating Species Distributions from eBird

Our first goal is to estimate $q_t(u)$, the fraction of birds in grid cell u during week t. Given enough observations, we are content to estimate $q_t(u)$ using the average number of birds per checklist, a quantity we call the *rate* $r_t(u)$. However, even for a bird with good eBird coverage, there are cells with few or no observations during a given time period. To fill these gaps, we use the *harmonic energy minimization* technique [12], which imposes a graph structure connecting the data according to similarity, and determines unknown values from nearby nodes in the graph. There are many possible interpretations of this technique [12, 13]; we describe it in terms of random walks.

The technique builds a weighted graph on data points z where edge weights $w_{zz'}$ represent similarity, and learns a function $f(z)$ on the points. Points with known values are boundary points and their value $f(z)$ is fixed; other points are interior points. For an interior point z, the value is determined as the expected value of the following random experiment. Perform a random walk starting from z, following outgoing edges with probability proportional to their weight. When a boundary point z' is reached, terminate the walk and accept the value $f(z')$. Interior points are influenced by boundary points in proportion to "nearness", as measured by the probability of hitting in an absorbing random walk. We derive a measure of confidence in $f(z)$ from the same experiment: let $h(z)$ be the expected number of steps for the random walk from z to hit the boundary (the *hitting time* of the boundary [14]). When $h(z)$ is small, z is close to the boundary so we are more confident in $f(z)$.

Our graph structure is a 3-dimensional lattice on the points u_t, where u_t represents cell u during week t. The connections for point u_t are illustrated in Figure 4. We exclude the edge between cells u_t, v_t when the line connecting the centers of u and v is more than half water. All edges have weight 1, except for edges connecting u_t to u_{t-1} and u_{t+1}, which have weight $1/4$, to prioritize spatial similarity over temporal similarity. All lattice points u_t are interior points; connected to u_t are boundary nodes for each observation with value equal to the number of birds observed. This achieves a "soft" boundary for lattice points: if u_t has many observations, the random walk from u_t will almost surely reach an observation in the first step, and $f(u_t)$ will be very close to $r_t(u)$, the average of the observations; nodes with few or no observations are more heavily influenced by neighbors. As a conservative measure, each node is also connected to a sink with boundary value 0, to prevent values from propagating over very long distances.

We compute h and f iteratively [13], taking $f(u_t)$ as an approximation for the rate $r_t(u)$, and multiplying by the land mass of cell u to get $\hat{q}_t(u)$, a (relative) estimate for the number of birds in each cell. Finally, since we want the fraction of birds from each time period in a given cell, we normalize $\hat{q}$ for each t, taking, $q_t(u) = \hat{q}_t(u) / \sum_u \hat{q}_t(u)$.

Figure 3: Range of Ruby-throated Hummingbird. From BNA [15].

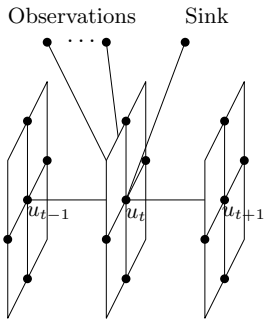

Figure 4: Illustration of local connectivity for lattice point u_t

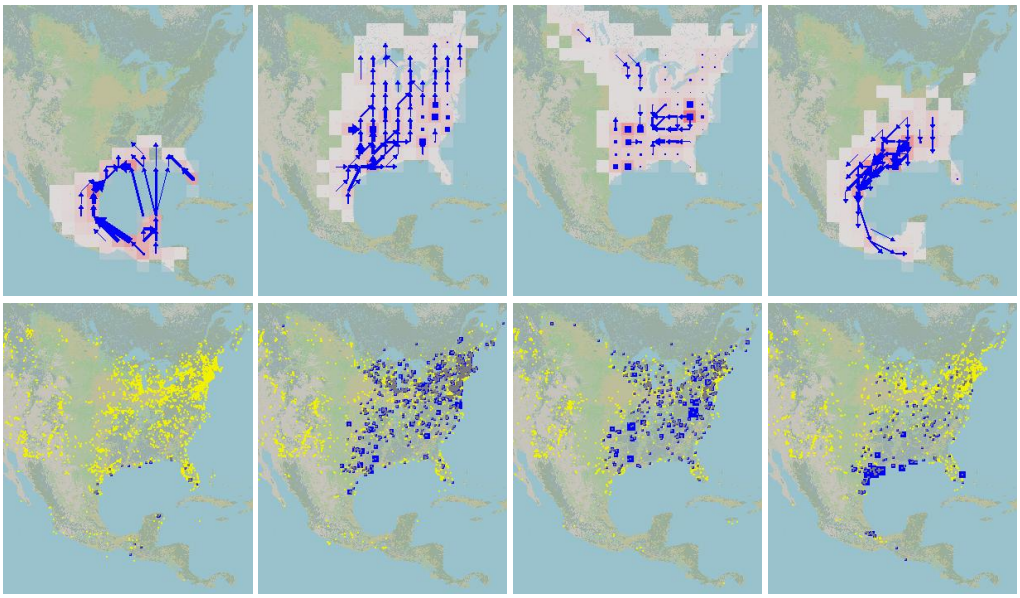

Figure 5: Ruby-throated Hummingbird migration. See text for description.

5.2 Migration Inference

Since the values for $q_t(u)$ are estimated, we introduce slack variables δ_u^t into the marginal constraints (5), obtaining

$$\sum_{u \in V_\alpha} \sum_{v \in V} x_{uv}^t = q_t(u) + \delta_u^t \qquad \text{for all } \alpha, t. \tag{5'}$$

To ensure that the new marginals $q'_t(u) = q_t(u) + \delta_u^t$ form a valid probability distribution for all t, we add constraints that $\sum_u \delta_u^t = 0$ for all t , and $\delta_u^t \geq -q_t(u)$ for all u, t, preserving the properties that q'_t is nonnegative and sums to 1. We also found it useful to impose upper bounds $\delta_u^t \leq 2q_t(u)$ so no single value can increase by more than a factor of 3. Finally, we add the term $\sum_{u,t} \gamma_u^t |\delta_u^t|$ into the objective function to charge for the slack, using a standard LP trick [8] to model the absolute value term.

For transition costs, we used squared distance (measured in pixels between grid cell centers): $c(u, v) = d(u, v)^2$, corresponding to Gaussian transition probabilities $p(u, v) \propto \exp(d(u, v)^2/\sigma^2)$. To reduce problem size, we omitted variables x_{uv}^t from the LP when $d(u, v) > 90$, effectively setting $p(u, v) = 0$. For the slack costs, we charged according to the confidence estimates $h(u_t)$ by setting $\gamma_u^t = \gamma_0/h(u_t)$ to be inversely proportional to hitting time, with $\gamma_0 \approx 261$ chosen so the av-

erage cost for a unit of slack was the same as moving 40 pixels. Our final linear program, which was solved using the MOSEK optimization toolbox, had $78{,}521$ constraints and $3{,}031{,}116$ variables.

Figure 5 displays the migration paths our model inferred for the Ruby-throated Hummingbird for the four weeks indicated. The top row shows the distribution and paths inferred by the model; grid cells colored in darker shades of red have more birds (higher values for $q'_t(u)$). Blue arrows indicate flight paths (x^t_{uv}) between the week shown and the following week, with line width in proportion to x^t_{uv}. In the bottom row, scatter plots of the raw data are given for comparison. Yellow dots indicate negative observations; blue squares indicate positive observations, with area proportional to count. Locations with both positive and negative observations appear dark gray.

These results are consitent with both seasonal ranges (Figure 3), and what is currently known about migration routes. In the summary paragraph on migration from the *Archilochus colubris* species account in Birds of North America, Robinson et al. write "Many fly across Gulf of Mexico, but many also follow coastal route. Routes may differ for north- and southbound birds." Our model for weeks 10 and 40 suggests that more southbound birds follow the coastal route.

6 Conclusion

Observational databases like eBird are a rich source of information about bird migration, but are static in nature and require inference to build dynamic migration models. Motivated by this problem, we developed an inference framework for Markov models that makes collective inferences about many independent sample paths drawn from a Markov chain. We demonstrated the effectiveness of our framework with results on the migration patterns of the Ruby-throated Hummingbird.

References

[1] L. R. Rabiner. A tutorial on hidden Markov models and selected applications in speech recognition. *Proceedings of the IEEE*, 77(2):257–286, 1989.

[2] E. Charniak. Statistical techniques for natural language parsing. *AI Magazine*, 18(4):33–44, 1997.

[3] R. Durbin, S. Eddy, A. Krogh, and G. Mitchison. *Biological sequence analysis: Probabilistic models of proteins and nucleic acids*. Cambridge University Press, 1998.

[4] R. Caruana, M. Elhawary, A. Munson, M. Riedewald, D. Sorokina, D. Fink, W. M. Hochachka, and S. Kelling. Mining citizen science data to predict prevalence of wild bird species. In *SIGKDD*, 2006.

[5] S. J. Phillips, M. Dudík, and R. E. Schapire. A maximum entropy approach to species distribution modeling. In *Proc. of ICML*, 2004.

[6] J. Lafferty, A. McCallum, and F. Pereira. Conditional random fields: Probabilistic models for segmenting and labeling sequence data. *Proc. of ICML*, 2001.

[7] D. Roth and W. Yih. Integer linear programming inference for conditional random fields. *Proc. of ICML*, 2005.

[8] V. Chvátal. *Linear Programming*. W.H. Freeman, New York, NY, 1983.

[9] A. V. Goldberg, S. A. Plotkin, and E. Tardos. Combinatorial algorithms for the generalized circulation problem. *Math. Oper. Res.*, 16(2):351–381, 1991.

[10] G. B. Dantzig. Application of the simplex method to a transportation problem. In T. C. Koopmans, editor, *Activity Analysis of Production and Allocation*, volume 13 of *Cowles Commission for Research in Economics*, pages 359–373. Wiley, 1951.

[11] J. Shore and R. Johnson. Properties of cross-entropy minimization. *IEEE Trans. on Information Theory*, 27:472–482, 1981.

[12] X. Zhu, Z. Ghahramani, and J. Lafferty. Semi-supervised learning using Gaussian fields and harmonic functions. In *Proc. of ICML*, 2003.

[13] P. G. Doyle and J. L. Snell. Random walks and electric networks. `http://www.citebase.org/abstract?id=oai:arXiv.org:math/0001057`, 2000.

[14] D. Aldous and J. Fill. *Reversible Markov Chains and Random Walks on Graphs*. Monograph in Preparation, `http://www.stat.berkeley.edu/users/aldous/RWG/book.html`.

[15] T. R. Robinson, R. R. Sargent, and M. B. Sargent. Ruby-throated Hummingbird (*Archilochus colubris*). In A. Poole and F. Gill, editors, *The Birds of North America*, number 204. The Academy of Natural Sciences, Philadelphia, and The American Ornithologists' Union, Washington, D.C., 1996.